Supersymmetric electroweak corrections to charged Higgs boson production in association with a top quark at hadron colliders

Li Gang Jin,[1] Chong Sheng Li,[1] Robert J. Oakes,[2] and Shou Hua Zhu[3,4]
[1]*Department of Physics, Peking University, Beijing 100871, China*
[2]*Department of Physics and Astronomy, Northwestern University, Evanston, Illinois 60208-3112*
[3]*CCAST (World Laboratory), Beijing 100080, China*
[4]*Institute of Theoretical Physics, Academia Sinica, Beijing 100080, China*
(Received 26 July 1999; revised manuscript received 15 December 1999; published 26 July 2000)

We calculate the $O(\alpha_{ew}m_{t(b)}^2/m_W^2)$ and $O(\alpha_{ew}m_{t(b)}^4/m_W^4)$ supersymmetric electroweak corrections to the cross section for charged Higgs boson production in association with a top quark at the Fermilab Tevatron and the CERN large hadron collider (LHC). These corrections arise from the quantum effects which are induced by potentially large Yukawa couplings from the Higgs sector and the chargino–top-quark– (bottom-quark–) bottom-squark (top-squark) couplings, neutralino–top-quark– (bottom-quark–) top-squark (bottom-squark) couplings and charged Higgs-boson–top-squark–bottom-squark couplings. They can decrease or increase the cross section depending on $\tan\beta$ but are not very sensitive to the mass of the charged Higgs boson for high $\tan\beta$. At low $\tan\beta(=2)$ the corrections decrease the total cross sections significantly, exceeding -12% for $m_{H^\pm}$ below 300 GeV at both the Tevatron and the LHC, but for $m_{H^\pm}>300$ GeV the corrections become very small at the LHC. For high $\tan\beta(=10,30)$ these corrections can decrease or increase the total cross sections, and the magnitude of the corrections are at most a few percent at both the Tevatron and the LHC.

PACS number(s): 14.80.Bn, 12.60.Jv, 13.85.Qk, 14.80.Cp

I. INTRODUCTION

There has been a great deal of interest in the charged Higgs bosons appearing in the two-Higgs-doublet models [1], particularly the minimal supersymmetric standard model (MSSM) [2], which predicts the existence of three neutral and two charged Higgs bosons h,H,A, and $H^\pm$. When the Higgs boson of the standard model (SM) has a mass below 130–140 GeV and the h boson of the MSSM is in the decoupling limit (which means that $H^\pm$ is too heavy anyway to possibly be produced), the lightest neutral Higgs boson may be difficult to distinguish from the neutral Higgs boson of the standard model (SM). But charged Higgs bosons carry a distinctive signature of the Higgs sector in the MSSM. Therefore, the search for charged Higgs bosons is very important for probing the Higgs sector of the MSSM and, therefore, will be one of the prime objectives of the CERN large hadron collider (LHC). At the LHC the integrated luminosity is expected to reach $L=100\ \text{fb}^{-1}$ per year in the second phase. Recently, several studies of charged Higgs boson production at hadron colliders have appeared in the literature [3–5]. For a relatively light charged Higgs boson, $m_{H^\pm}<m_t-m_b$, the dominate production processes at the LHC are $gg\to t\bar{t}$ and $q\bar{q}\to t\bar{t}$ followed by the decay sequence $t\to bH^+\to b\tau^+\nu_\tau$ [6]. For a heavier charged Higgs boson the dominate production process is $gb\to tH^-$ [7–9]. Previous studies showed that the search for heavy charged Higgs bosons with $m_{H^\pm}>m_t+m_b$ at a hadron collider is seriously complicated by QCD backgrounds due to processes such as $gb\to t\bar{t}b$, $g\bar{b}\to t\bar{t}\bar{b}$, and $gg\to t\bar{t}b\bar{b}$, as well as other processes [8]. However, recent analyses [10,11] indicate that the decay mode $H^+\to\tau^+\nu$ provides an excellent signature for a heavy charged Higgs boson in searches at the LHC. The discovery region for $H^\pm$ is far greater than had been thought for a large range of the $(m_{H^\pm},\tan\beta)$ parameter space, extending beyond $m_{H^\pm}\sim1$ TeV and down to at least $\tan\beta\sim3$, and potentially to $\tan\beta\sim1.5$, assuming the latest results for the SM parameters and parton distribution functions as well as using kinematic selection techniques and the τ polarization analysis [11]. Of course, it is just a theoretical analysis and no experimental simulation has been performed to make the statement very reliable so far.

The one-loop radiative corrections to H^-t associated production have not been calculated, although this production process has been studied extensively at tree level [7–9]. In this paper we present the calculations of the $O(\alpha_{ew}m_{t(b)}^2/m_W^2)$ and $O(\alpha_{ew}m_{t(b)}^4/m_W^4)$ supersymmetric (SUSY) electroweak corrections to this associated H^-t production process at both the Fermilab Tevatron and the LHC in the MSSM. These corrections arise from the quantum effects which are induced by potentially large Yukawa couplings from the Higgs sector and the chargino-top-quark (bottom-quark–) bottom-squark (top-squark) couplings, neutralino-top-quark (bottom-quark–) bottom-squark (top-squark) couplings, and charged Higgs-boson–top-squark–bottom-squark couplings which will contribute at the $O(\alpha_{ew}m_{t(b)}^4/m_W^4)$ to the self-energy of the charged Higgs boson. In order to get a reliable estimate this process has to be merged with the related gluon splitting contribution $gg\to H^-t\bar{b}$. This leads to a suppression by about 50% at LO [12]. However, the complete one-loop QCD corrections are probably more important, but not yet available.

II. CALCULATIONS

The tree-level amplitude for $gb\to tH^-$ is

$$M_0=M_0^{(s)}+M_0^{(t)}, \tag{1}$$

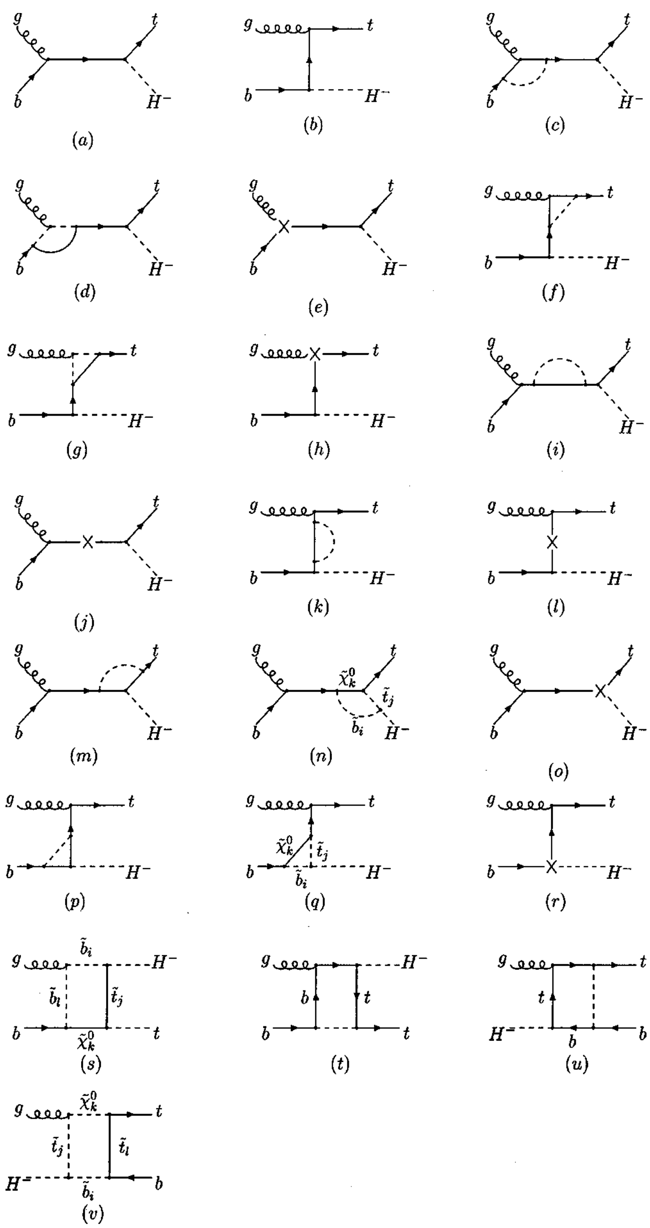

FIG. 1. Feynman diagrams contributing to $O(\alpha_{ew}m_{t(b)}^2/m_W^2)$ Yukawa corrections to $gb\rightarrow tH^-$: (a) and (b) are tree-level diagrams; (c)–(v) are one-loop diagrams. The dashed lines represent H, h, A, $H^{\pm}$, G^0, and $G^{\pm}$ for diagrams (c) and (f); H, h, A, and G^0 for diagrams (m), (p) (t), and (u); $\tilde{t}$, $\tilde{b}$, H, h, A, $H^{\pm}$, G^0 and $G^{\pm}$ for (i) and (k), where the solid lines represent charginos and neutralinos if the dashed lines represent squarks. For diagrams (d) and (g), the solid lines in the loop represent $\tilde{\chi}^0$ and $\tilde{\chi}^+$ and the dashed lines represent squarks.

where $M_0^{(s)}$ and $M_0^{(t)}$ represent the amplitudes arising from diagrams in Figs. 1(a) and 1(b), respectively. Explicitly,

$$M_0^{(s)}=\frac{igg_s}{\sqrt{2}m_W(\hat{s}-m_b^2)}\overline{u}(p_t)[2m_t\cot\beta p_b^{\mu}P_L+2m_b\tan\beta p_b^{\mu}P_R-m_t\cot\beta\gamma^{\mu}\not{k}P_L-m_b\tan\beta\gamma^{\mu}\not{k}P_R]u(p_b)\varepsilon_{\mu}(k)T_{ij}^a, \qquad (2)$$

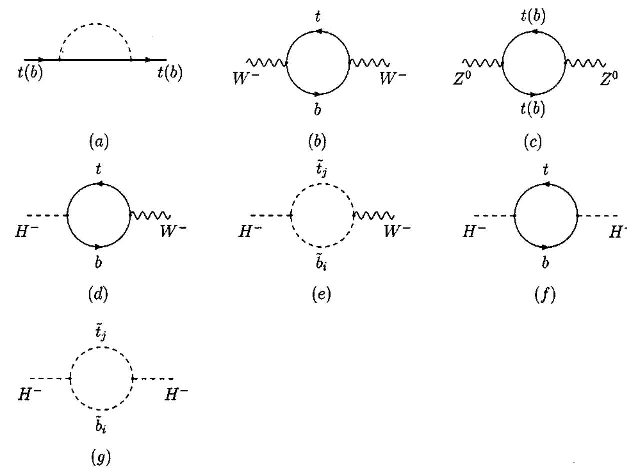

FIG. 2. Self-energy Feynman diagrams contributing to renormalization constants: The dashed lines represent $\tilde{t}$, $\tilde{b}$, H, h, A, $H^{\pm}$, G^0, and $G^{\pm}$ for diagam (a), where the solid lines represent charginos and neutralinos if the dashed lines represent squarks.

and

$$M_0^{(t)}=\frac{igg_s}{\sqrt{2}m_W(\hat{t}-m_t^2)}\overline{u}(p_t)[2m_t\cot\beta p_t^{\mu}P_L+2m_b\tan\beta p_t^{\mu}P_R-m_t\cot\beta\gamma^{\mu}\not{k}P_L-m_b\tan\beta\gamma^{\mu}\not{k}P_R]u(p_b)\varepsilon_{\mu}(k)T_{ij}^a, \qquad (3)$$

where T^a are the $SU(3)$ color matrices and $\hat{s}$ and $\hat{t}$ are the subprocess Mandelstam variables defined by

$$\hat{s}=(p_b+k)^2=(p_t+p_{H^-})^2,$$

and

$$\hat{t}=(p_t-k)^2=(p_{H^-}-p_b)^2.$$

Here the Cabibbo-Kobayashi-Maskawa (CKM) matrix element $V_{CKM}[bt]$ has been taken to be unity.

The SUSY electroweak corrections of order $O(\alpha_{ew}m_{t(b)}^2/m_W^2)$ and $O(\alpha_{ew}m_{t(b)}^4/m_W^4)$ to the process $gb\rightarrow H^-t$ arise from the Feynman diagrams shown in Figs. 1(c)–1(v) and Fig. 2. We carried out the calculation in the 't Hooft–Feynman gauge and used dimensional reduction, which preserves supersymmetry, for regularization of the ultraviolet divergences in the virtual loop corrections using the on-mass-shell renormalization scheme [13], in which the fine-structure constant α_{ew} and physical masses are chosen to be the renormalized parameters, and finite parts of the counterterms are fixed by the renormalization conditions. The coupling constant g is related to the input parameters e, m_W, and m_Z by $g^2=e^2/s_w^2$ and $s_w^2=1-m_w^2/m_Z^2$. The parameter β in the MSSM we are considering must also be renormalized. Following the analysis of Ref. [14], this renormalization constant was fixed by the requirement that the on-mass-shell $H^+\overline{l}\nu_l$ coupling remain the same form as in Eq. (2) of Ref. [14] to all orders of perturbation theory. Taking into account the $O(\alpha_{ew}m_{t(b)}^2/m_W^2)$ and $O(\alpha_{ew}m_{t(b)}^4/m_W^4)$ SUSY electroweak corrections, the renormalized amplitude for the process $gb\to tH^-$ can be written as

$$M_{ren}=M_0^{(s)}+M_0^{(t)}+\delta M^{V_1(s)}+\delta M^{V_1(t)}+\delta M^{s(s)}+\delta M^{s(t)}+\delta M^{V_2(s)}+\delta M^{V_2(t)}+\delta M^{b(s)}+\delta M^{b(t)}\equiv M_0^{(s)}+M_0^{(t)}+\sum_l \delta M^l, \quad (4)$$

where $\delta M^{V_1(s)}$, $\delta M^{V_1(t)}$, $\delta M^{s(s)}$, $\delta M^{s(t)}$, $\delta M^{V_2(s)}$, $\delta M^{V_2(t)}$, $\delta M^{b(s)}$, and $\delta M^{b(t)}$ represent the corrections to the tree diagrams arising, respectively, from the gbb vertex diagram Figs. 1(c) and 1(d), the gtt vertex diagram Figs. 1(f) and 1(g), the bottom-quark self-energy diagram Fig. 1(i), the top-quark self-energy diagram Fig. 1(k), the btH^- vertex diagrams Figs. 1(m) and 1(n) and Figs. 1(p) and 1(q), including their corresponding counterterms Figs. 1(e), 1(h), 1(j), 1(l), 1(o), and 1(r), and the box diagrams Figs. 1(s)–1(v). $\Sigma_l\delta M^l$ then represents the sum of the contributions to the SUSY electroweak corrections from all the diagrams in Figs. 1(c)–1(v). The explicit form of δM^l can be expressed as

$$\delta M^l=-\frac{ig^3g_sT_{ij}^a}{4\sqrt{2}\times 16\pi^2 m_W}C^l\overline{u}(p_t)\{f_1^l\gamma^\mu P_L+f_2^l\gamma^\mu P_R+f_3^lp_b^\mu P_L+f_4^lp_b^\mu P_R+f_5^lp_t^\mu P_L+f_6^lp_t^\mu P_R+f_7^l\gamma^\mu \not{k}P_L+f_8^l\gamma^\mu\not{k}P_R+f_9^lp_b^\mu\not{k}P_L+f_{10}^lp_b^\mu\not{k}P_R+f_{11}^lp_t^\mu\not{k}P_L+f_{12}^lp_t^\mu\not{k}P_R\}u(p_b)\varepsilon_\mu(k), \quad (5)$$

where the C^l are coefficients that depend on $\hat{s},\hat{t}$, and the masses, and the f_i^l are form factors; both the coefficients C^l and the form factors f_i^l are given explicitly in Appendix A. The corresponding amplitude squared is

$$\overline{\sum}|M_{ren}|^2=\overline{\sum}|M_0^{(s)}+M_0^{(t)}|^2+2\,\mathrm{Re}\overline{\sum}\left[\left(\sum_l\delta M^l\right)(M_0^{(s)}+M_0^{(t)})^\dagger\right], \quad (6)$$

where

$$\overline{\sum}|M_0^{(s)}+M_0^{(t)}|^2=\frac{g^2g_s^2}{2N_Cm_W^2}\left\{\frac{1}{(\hat{s}-m_b^2)^2}[(m_t^2\cot^2\beta+m_b^2\tan^2\beta)(p_b\cdot kp_t\cdot k-m_b^2p_t\cdot k+2p_b\cdot kp_b\cdot p_t-m_b^2p_b\cdot p_t)+2m_b^2m_t^2(p_b\cdot k-m_b^2)]+\frac{1}{(\hat{t}-m_t^2)^2}[(m_t^2\cot^2\beta+m_b^2\tan^2\beta)(p_b\cdot kp_t\cdot k+m_t^2p_b\cdot k-m_t^2p_b\cdot p_t)+2m_b^2m_t^2(p_t\cdot k-m_t^2)]+\frac{1}{(\hat{s}-m_b^2)(\hat{t}-m_t^2)}[(m_t^2\cot^2\beta+m_b^2\tan^2\beta)(2p_b\cdot kp_t\cdot k+2p_b\cdot kp_b\cdot p_t-2(p_b\cdot p_t)^2-m_b^2p_t\cdot k+m_t^2p_b\cdot k)+2m_b^2m_t^2(p_t\cdot k-p_b\cdot k-2p_b\cdot p_t)]\right\}, \quad (7)$$

$$\overline{\sum}\delta M^l(M_0^{(s)})^\dagger=-\frac{g^4g_s^2}{64N_C\times 16\pi^2m_W^2(\hat{s}-m_b^2)}C^l\sum_{i=1}^{12}h_i^{(s)}f_i^l, \quad (8)$$

and

$$\overline{\sum}\delta M^l(M_0^{(t)})^\dagger=-\frac{g^4g_s^2}{64N_C\times 16\pi^2m_W^2(\hat{t}-m_t^2)}C^l\sum_{i=1}^{12}h_i^{(t)}f_i^l. \quad (9)$$

Here the color factor $N_C=3$ and $h_i^{(s)}$ and $h_i^{(t)}$ are scalar functions whose explicit expressions are given in Appendix B.

The cross section for the process $gb\to tH^-$ is

$$\hat{\sigma}=\int_{\hat{t}_{min}}^{\hat{t}_{max}}\frac{1}{16\pi\hat{s}^2}\overline{\Sigma}|M_{ren}|^2d\hat{t} \quad (10)$$

with

$$\hat{t}_{min}=\frac{m_t^2+m_{H^-}^2-\hat{s}}{2}-\frac{1}{2}\sqrt{[\hat{s}-(m_t+m_{H^-})^2][\hat{s}-(m_t-m_{H^-})^2]},$$

and

$$\hat{t}_{max}=\frac{m_t^2+m_{H^-}^2-\hat{s}}{2}+\frac{1}{2}\sqrt{[\hat{s}-(m_t+m_{H^-})^2][\hat{s}-(m_t-m_{H^-})^2]}.$$

The total hadronic cross section for $pp\to gb\to tH^-$ can be obtained by folding the subprocess cross section $\hat{\sigma}$ with the parton luminosity:

$$\sigma(s)=\int_{(m_t+m_{H^-})/\sqrt{s}}^{1}dz\frac{dL}{dz}\hat{\sigma}(gb\to tH^- \text{ at } \hat{s}=z^2s). \tag{11}$$

Here $\sqrt{s}$ and $\sqrt{\hat{s}}$ are the c.m. energies of the pp and gb states, respectively, and dL/dz is the parton luminosity, defined as

$$\frac{dL}{dz}=2z\int_{z^2}^{1}\frac{dx}{x}f_{b/P}(x,\mu)f_{g/P}(z^2/x,\mu), \tag{12}$$

where $f_{b/P}(x,\mu)$ and $f_{g/P}(z^2/x,\mu)$ are the bottom-quark and gluon parton distribution functions.

III. NUMERICAL RESULTS AND CONCLUSION

In the following we present some numerical results for charged Higgs-boson production in association with a top quark at both the Tevatron and the LHC. In our numerical calculations the SM parameters were taken to be $m_W=80.41$ GeV, $m_Z=91.187$ GeV, $m_t=176$ GeV, $\alpha_s(m_Z)=0.119$, and $\alpha_{ew}(m_Z)=\frac{1}{128.8}$ [15]. And we used the running b-quark mass 3 GeV and the one-loop relations [16] from the MSSM between the Higgs boson masses $m_{h,H,A,H^\pm}$ and the parameters α and β, and chose $m_{H^\pm}$ and $\tan\beta$ as the two independent input parameters. And we used the CTEQ5M [17] parton distributions throughout the calculations. Other MSSM parameters were determined as follows:

(i) For the parameters M_1, M_2, and μ in the chargino and neutralino matrix, we set $M_2=300$ GeV and then used the relation $M_1=(5/3)(g'^2/g^2)M_2\simeq 0.5M_2$ [2] to determine M_1. We also set $\mu=-100$ GeV except for the numerical calculations shown in Fig. 6(b), where μ is a variable.

(ii) For the parameters $m^2_{\tilde{Q},\tilde{U},\tilde{D}}$ and $A_{t,b}$ in squark mass matrices

$$M^2_{\tilde{q}}=\begin{pmatrix} M^2_{LL} & m_qM_{LR} \\ m_qM_{RL} & M^2_{RR}\end{pmatrix} \tag{13}$$

with

$$M^2_{LL}=m^2_{\tilde{Q}}+m_q^2+m_Z^2\cos 2\beta(I_q^{3L}-e_q\sin^2\theta_W),$$

$$M^2_{RR}=m^2_{\tilde{U},\tilde{D}}+m_q^2+m_Z^2\cos 2\beta e_q\sin^2\theta_W,$$

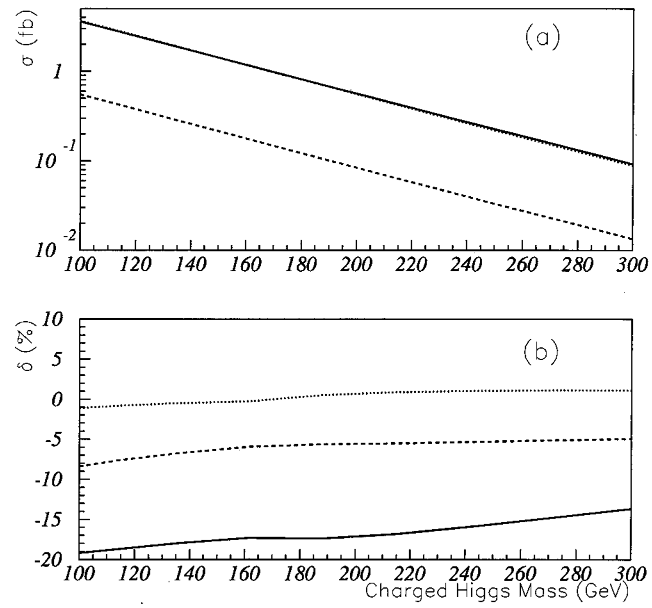

FIG. 3. The tree-level total cross sections (a) and relative one-loop corrections (b) versus $m_{H^\pm}$ at the Tevatron with $\sqrt{s}=2$ TeV. The solid, dashed, and dotted lines correspond to $\tan\beta=2$, 10, and 30, respectively.

$$M_{LR}=M_{RL}=\begin{pmatrix} A_t-\mu\cot\beta & (\tilde{q}=\tilde{t}) \\ A_b-\mu\tan\beta & (\tilde{q}=\tilde{b})\end{pmatrix}, \tag{14}$$

to simplify the calculation we assumed $m^2_{\tilde{Q}}=m^2_{\tilde{U}}=m^2_{\tilde{D}}$ and $A_t=A_b$, and we set $m_{\tilde{Q}}=500$ GeV and $A_t=200$ GeV. But in the numerical calculations of Fig. 6(a) $A_t=A_b$ are the variables.

Some typical numerical calculations of the tree-level total cross sections and the $O(\alpha_{ew}m^2_{t(b)}/m^2_W)$ and $O(\alpha_{ew}m^4_{t(b)}/m^4_W)$ SUSY electroweak corrections as the functions of the charged Higgs-boson mass, $A_t=A_b$ and μ, respectively, for three representative values of $\tan\beta$ are given in Figs. 3–6.

Figures 3(a) and 4(a) show that the tree-level total cross sections as a function of the charged Higgs boson mass for three representative values of $\tan\beta$. For $m_{H^\pm}=200$ GeV the total cross sections at the Tevatron are at most only 0.7 and 0.1 fb for $\tan\beta=2$, 30, and 10, respectively, and for $m_{H^\pm}=300$ GeV the total cross sections are smaller than 0.15 fb for all three values of $\tan\beta$. However, at the LHC the total cross sections are much larger: the order of thousands of fb for $m_{H^\pm}$ in the range 100–240 GeV and $\tan\beta=2$ and 30; and they are hundreds of fb for the intermediate value $\tan\beta=10$. When the charged Higgs boson mass becomes heavy (<500 GeV), the total cross sections still are larger than 100 and 10 fb for $\tan\beta=2$, 30, and 10, respectively. For low $\tan\beta$ the top-quark contribution is enhanced, while for high $\tan\beta$ the bottom-quark contribution becomes large. These results are smaller than ones given in Refs. [8,9] because we used the running b quark mass 3 GeV in the numerical calculations. We have confirmed that if we chose $m_b=4.5$ GeV, our results will agree with Refs. [8,9].

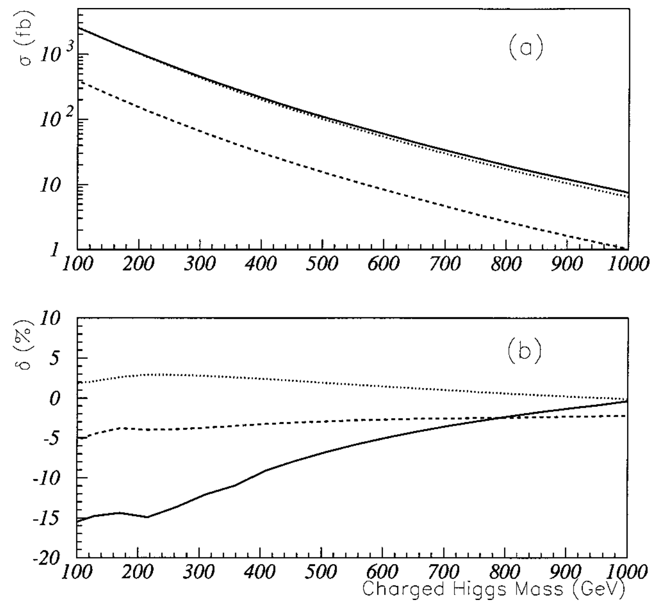

FIG. 4. The tree-level total cross sections (a) and relative one-loop corrections (b) versus $m_{H^\pm}$ at the LHC with $\sqrt{s}=4$ TeV. The solid, dashed, and dotted lines correspond to $\tan\beta=2$, 10, and 30, respectively.

In Figs. 3(b) and 4(b) we show the corrections to the total cross sections relative to the tree-level values as a function of $m_{H^\pm}$ for $\tan\beta=2$, 10, and 30. For $\tan\beta=2$ the corrections decrease the total cross sections significantly, exceeding -13% for $m_{H^\pm}$ below 300 GeV at the both Tevatron and the LHC. But the corrections decrease as $m_{H^\pm}$ increase. For example, as shown in Fig. 4(b), the corrections range between -13% and $\sim 0\%$ when $m_{H^\pm}$ increase from 300 GeV to 1 TeV at the LHC. For high $\tan\beta(=10{,}30)$ these corrections become smaller, which can decrease or increase the total cross sections depending on $\tan\beta$, and the magnitude of the corrections are at most a few percent for a wide range of the charged Higgs boson mass at both the Tevatron and the LHC.

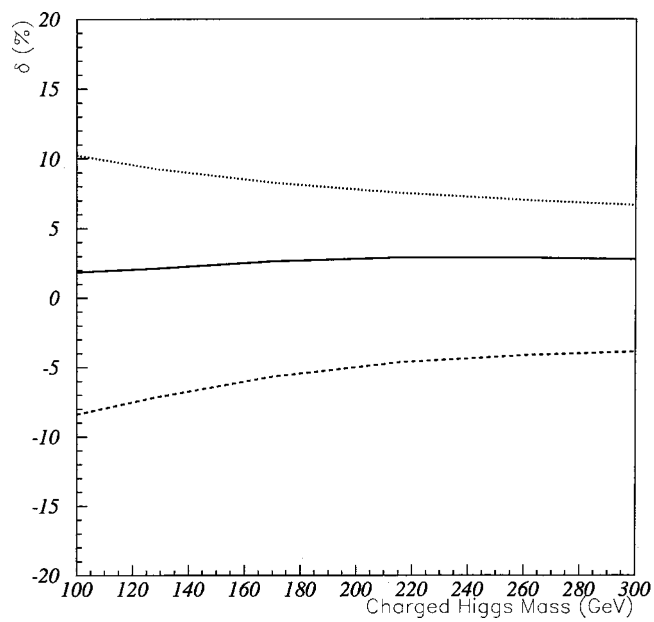

FIG. 5. The radiative correction from top, bottom quarks (dashed line) and genuine SUSY particles (dotted line), as well as total contributions (solid line) when $\tan\beta=30$ at the LHC with $\sqrt{s}=14$ TeV.

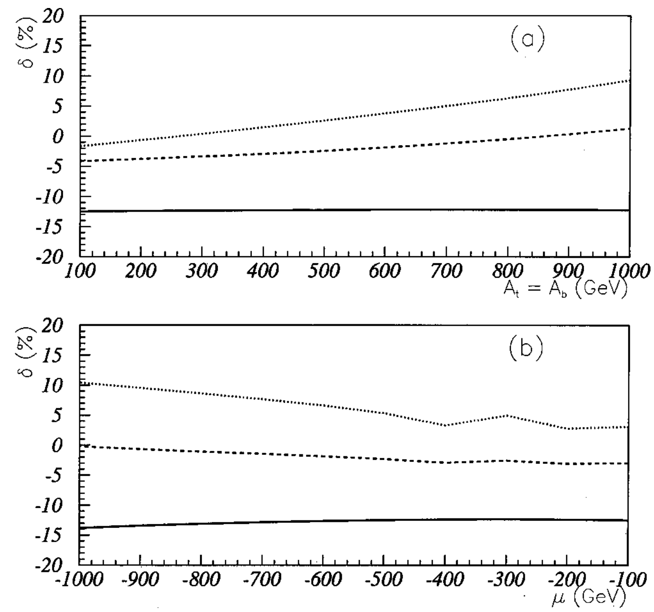

FIG. 6. Relative one-loop corrections versus A_t, A_b (a) as well as μ (b) at the LHC with $\sqrt{s}=14$ TeV, where $m_{H^\pm}=300$ GeV and the solid, dashed, and dotted lines correspond to $\tan\beta=2$, 10, and 30, respectively. For (a), $\mu=-100$ GeV, and for (b), $A_t=A_b=200$ GeV.

In Fig. 5 we present the Yukawa correction from the Higgs sector and the genuine SUSY electroweak correction from the couplings involving the genuine SUSY particles (the chargino, neutralino, and squark) for $\tan\beta=30$ at the LHC, respectively. One can see that the Yukawa correction and the genuine SUSY electroweak correction have opposite signs, and thus cancel to some extent. The former decrease the total cross sections, which can range between -8% and $\sim -4\%$ for $m_{H^\pm}$ below 300 GeV, but the latter increase the total cross sections, which range between 10% and $\sim 7\%$ for $m_{H^\pm}$ in the same range. In such a case the combined effects just are about 2% and $\sim 3\%$.

Figures 6(a) and 6(b) give the corrections as the functions of $A_t=A_b$ and μ for $m_{H^\pm}=300$ GeV at the LHC, respectively, assuming $\tan\beta=2$, 10, and 30. From Figs. 6(a) and 6(b) one sees that the corrections increase or decrease slowly with increasing $A_t=A_b$ and the magnitude of μ, respectively, for $\tan\beta=30{,}10$, and the corrections are not very sensitive to either $A_t=A_b$ or μ for $\tan\beta=2$, where the corrections are always about -12% and -13%, respectively. In general, for large values of A_t and small values of $\tan\beta$ or large values of μ and $\tan\beta$, one finds much larger corrections since the charged Higgs-boson–top-squark–bottom-squark couplings become stronger. For $\tan\beta=30$, comparing Fig. 4(b) with Fig. 6(b), we can see that the corrections indeed become larger as the values of μ increase. But for

$\tan\beta=2$ from Fig. 4(a) and Fig. 6(a) we found that the corrections change very little when $A_t=A_b$ becomes larger. Obviously, the effects of the stronger couplings have been suppressed by decoupling effects because with an increase of $A_t=A_b$ all the squark masses are still heavy, which is almost the same situation discussed in Ref. [18].

In conclusion, we have calculated the $O(\alpha_{ew}m_{t(b)}^2/m_W^2)$ and $O(\alpha_{ew}m_{t(b)}^4/m_W^4)$ SUSY electroweak corrections to the cross section for the charged Higgs-boson production in association with a top quark at the Tevatron and the LHC. These corrections decrease or increase the cross section depending on $\tan\beta$ but are not very sensitive to the mass of the charged Higgs boson for high $\tan\beta$. At low $\tan\beta(=2)$ the corrections decrease the total cross sections significantly, exceeding -12% for $m_{H^\pm}$ below 300 GeV at both the Tevatron and the LHC, but for $m_{H^\pm}>300$ GeV the corrections become small at the LHC. For high $\tan\beta(=10,30)$ these corrections can decrease or increase the total cross sections, and the magnitude of the corrections are at most a few percent at both the Tevatron and the LHC.

ACKNOWLEDGMENTS

This work was supported in part by the National Natural Science Foundation of China, the Doctoral Program Foundation of Higher Education of China, the Post Doctoral Foundation of China, a grant from the State Commission of Science and Technology of China, and the U.S. Department of Energy, Division of High Energy Physics, under Grant No. DE-FG02-91-ER4086. S.H. Zhu also gratefully acknowledges the support of the K.C. Wong Education Foundation of Hong Kong.

APPENDIX A

The coefficients C^l and form factors f_i^l are the following:

$$C^{V_1(s)}=\frac{m_b^2}{m_W^2(\hat{s}-m_b^2)},\quad C^{V_1(t)}=\frac{m_t^2}{m_W^2(\hat{t}-m_t^2)},\quad C^{s(s)}=\frac{m_b^2}{m_W^2(\hat{s}-m_b^2)^2},$$

$$C^{s(t)}=\frac{m_t^2}{m_W^2(\hat{t}-m_t^2)^2},\quad C^{V_2(s)}=\frac{m_bm_t}{m_W^2(\hat{s}-m_b^2)},C^{V_2(t)}=\frac{m_bm_t}{m_W^2(\hat{t}-m_t^2)},$$

$$C^{b(s)}=C^{b(t)}=\frac{m_tm_b}{m_W^2},$$

$$f_1^{V_1(s)}=\eta^{(1)}[m_b(g_2^{V_1(s)}-g_3^{V_1(s)})-2p_b\cdot kg_6^{V_1(s)}],$$

$$f_2^{V_1(s)}=\eta^{(2)}[m_b(g_3^{V_1(s)}-g_2^{V_1(s)})-2p_b\cdot kg_7^{V_1(s)}],$$

$$f_3^{V_1(s)}=\eta^{(2)}[2(g_1^{V_1(s)}+g_2^{V_1(s)})+m_b(g_4^{V_1(s)}+g_5^{V_1(s)})+2p_b\cdot kg_8^{V_1(s)}],$$

$$f_4^{V_1(s)}=\eta^{(1)}[2(g_1^{V_1(s)}+g_3^{V_1(s)})+m_b(g_4^{V_1(s)}+g_5^{V_1(s)})+2p_b\cdot kg_9^{V_1(s)}],$$

$$f_7^{V_1(s)}=\eta^{(2)}[-(g_1^{V_1(s)}+g_2^{V_1(s)})+m_b(g_6^{V_1(s)}+g_7^{V_1(s)})],$$

$$f_8^{V_1(s)}=\eta^{(1)}[-(g_1^{V_1(s)}+g_3^{V_1(s)})+m_b(g_6^{V_1(s)}+g_7^{V_1(s)})],$$

$$f_9^{V_1(s)}=\eta^{(1)}[g_4^{V_1(s)}+2g_6^{V_1(s)}+m_b(g_8^{V_1(s)}-g_9^{V_1(s)})],$$

$$f_{10}^{V_1(s)}=\eta^{(2)}[g_5^{V_1(s)}+2g_7^{V_1(s)}+m_b(g_9^{V_1(s)}-g_8^{V_1(s)})],$$

$$f_1^{V_2(s)}=2p_b\cdot kg_3^{V_2(s)},\quad f_2^{V_2(s)}=2p_b\cdot kg_4^{V_2(s)},$$

$$f_3^{V_2(s)}=2g_1^{V_2(s)}+2m_t\cot\beta(\delta\Lambda_L^{(1)}+\delta\Lambda_L^{(2)}+\delta\Lambda_L^{(3)})-2m_tg_3^{V_2(s)}+2m_bg_4^{V_2(s)},$$

$$f_4^{V_2(s)}=2g_2^{V_2(s)}+2m_b\tan\beta(\delta\Lambda_R^{(1)}+\delta\Lambda_R^{(2)}+\delta\Lambda_R^{(3)})+2m_bg_3^{V_2(s)}-2m_tg_4^{V_2(s)},$$

$$f_7^{V_2(s)}=-\frac{1}{2}f_3^{V_2(s)},\quad f_8^{V_2(s)}=-\frac{1}{2}f_4^{V_2(s)},$$

$$f_1^{V_2(t)}=2p_t\cdot k g_3^{V_2(t)},\quad f_2^{V_2(t)}=2p_t\cdot k g_4^{V_2(t)},$$

$$f_5^{V_2(t)}=2g_1^{V_2(t)}+2m_t\cot\beta(\delta\Lambda_L^{(1)}+\delta\Lambda_L^{(2)}+\delta\Lambda_L^{(3)})-2m_tg_3^{V_2(t)}+2m_bg_4^{V_2(t)},$$

$$f_6^{V_2(t)}=2g_2^{V_2(t)}+2m_b\tan\beta(\delta\Lambda_R^{(1)}+\delta\Lambda_R^{(2)}+\delta\Lambda_R^{(3)})+2m_bg_3^{V_2(t)}-2m_tg_4^{V_2(t)},$$

$$f_7^{V_2(t)}=-\frac{1}{2}f_5^{V_2(t)},\quad f_8^{V_2(t)}=-\frac{1}{2}f_6^{V_2(t)},$$

$$f_1^{s(s)}=2\eta^{(1)}p_b\cdot k[g_1^{s(s)}+m_b(g_2^{s(s)}+g_3^{s(s)})],$$

$$f_2^{s(s)}=2\eta^{(2)}p_b\cdot k[g_5^{s(s)}+m_b(g_2^{s(s)}+g_4^{s(s)})],$$

$$f_3^{s(s)}=2\eta^{(2)}[m_b(g_1^{s(s)}+g_5^{s(s)})+2(m_b^2+p_b\cdot k)g_2^{s(s)}+(m_b^2+2p_b\cdot k)g_3^{s(s)}+m_b^2g_4^{s(s)}],$$

$$f_4^{s(s)}=2\eta^{(1)}[m_b(g_1^{s(s)}+g_5^{s(s)})+2(m_b^2+p_b\cdot k)g_2^{s(s)}+m_b^2g_3^{s(s)}+(m_b^2+2p_b\cdot k)g_4^{s(s)}],$$

$$f_7^{s(s)}=-\frac{1}{2}f_3^{s(s)},\quad f_8^{s(s)}=-\frac{1}{2}f_4^{s(s)},$$

$$\begin{aligned}f_1^{b(s)}=&\sum_{i=H^0,h^0,G^0,A^0}\eta_i^{(3)}\{\eta^{(2)}[2m_b(-3D_{312}+(1-\zeta_i)D_{27})+m_b^3(D_0+D_{12}-D_{22}-D_{32})-m_t^2m_b(D_{23}+2D_{39})\\&-2m_bp_b\cdot k(2D_{36}+D_{24}+\zeta_i(D_0+D_{12}))+2m_bp_t\cdot k(D_{25}+D_{310})+2m_bp_b\cdot p_t(D_{26}+2D_{38})]+\eta^{(1)}[2m_t(-3D_{313}\\&+(1+\zeta_i)D_{27})-m_t^3(D_{33}+(1+\zeta_i)D_{23})+m_b^2m_t(D_{13}-2D_{38}+(1+\zeta_i)(D_0-D_{22}))+2m_tp_b\cdot k(D_{13}-D_{310}-(1\\&+\zeta_i)(D_{12}+D_{24}))+2m_tp_t\cdot k(2D_{37}+(1+\zeta_i)D_{25})+2m_tp_b\cdot p_t(2D_{39}+(1+\zeta_i)D_{26})]\}(-k,\\&-p_b,p_t,m_b,m_b,m_i,m_t)-\frac{8\sqrt{2}m_W}{\sin 2\beta}\sum_{i,j,k}N_{k4}N_{k3}^*R_i(b)R_j(t)\sigma_{ij}D_{27}(-k,-p_b,p_t,m_{\tilde b_i},m_{\tilde b_i},m_{\tilde\chi_k^0},m_{\tilde t_j}),\end{aligned}$$

$$f_2^{b(s)}=f_1^{b(s)}(\eta^{(1)}\leftrightarrow\eta^{(2)},L_l\leftrightarrow R_l,N_{kl}\leftrightarrow N_{kl}^*),$$

$$\begin{aligned}f_3^{b(s)}=&\sum_{i=H^0,h^0,G^0,A^0}\eta_i^{(3)}\{\eta^{(1)}[-4D_{27}+2m_b^2(D_{22}-D_0-(1-\zeta_i)(D_{12}+D_{22}))\\&+2m_t^2(D_{23}-(1+\zeta_i)D_{26})+4p_t\cdot k(D_{26}-D_{25})]+\eta^{(2)}2m_tm_b(1+\zeta_i)(D_{22}-D_{12}-D_{26})\}\\&\times(-k,-p_b,p_t,m_b,m_b,m_i,m_t)-\frac{8\sqrt{2}m_W}{\sin 2\beta}\sum_{i,j,k}\sigma_{ij}[-m_tN_{k4}N_{k3}^*R_i(b)R_j(t)D_{26}\\&+m_bN_{k4}^*N_{k3}L_i(b)L_j(t)(D_{12}+D_{22})+m_{\tilde\chi_k^0}N_{k4}^*N_{k3}^*R_i(b)L_j(t)D_{12}](-k,-p_b,p_t,m_{\tilde b_i},m_{\tilde b_i},m_{\tilde\chi_k^0},m_{\tilde t_j}),\end{aligned}$$

$$f_4^{b(s)}=f_3^{b(s)}(\eta^{(1)}\leftrightarrow\eta^{(2)},L_l\leftrightarrow R_l,N_{kl}\leftrightarrow N_{kl}^*),$$

$$\begin{aligned}f_5^{b(s)}=&\sum_{i=H^0,h^0,G^0,A^0}\eta_i^{(3)}\{\eta^{(1)}[12D_{313}+2m_b^2(2D_{38}-D_{13}+(1-\zeta_i)(D_{13}+D_{26}))+2m_t^2(D_{33}+(1+\zeta_i)D_{23})\\&+4p_b\cdot k(D_{25}+D_{310})-4p_t\cdot k(D_{23}+2D_{37})-4p_t\cdot p_b(D_{23}+2D_{39})]+\eta^{(2)}2m_tm_b(1+\zeta_i)(D_{13}+D_{23}-D_{26})\}\\&\times(-k,-p_b,p_t,m_b,m_b,m_i,m_t)+\frac{8\sqrt{2}m_W}{\sin 2\beta}\sum_{i,j,k}\sigma_{ij}[-m_tN_{k4}N_{k3}^*R_i(b)R_j(t)D_{23}\\&+m_bN_{k4}^*N_{k3}L_i(b)L_j(t)(D_{13}+D_{26})+m_{\tilde\chi_k^0}N_{k4}^*N_{k3}^*R_i(b)L_j(t)D_{13}](-k,-p_b,p_t,m_{\tilde b_i},m_{\tilde b_i},m_{\tilde\chi_k^0},m_{\tilde t_j}),\end{aligned}$$

$$f_6^{b(s)}=f_5^{b(s)}(\eta^{(1)}\leftrightarrow\eta^{(2)},L_l\leftrightarrow R_l,N_{kl}\leftrightarrow N_{kl}^*),$$

$$f_7^{b(s)}=\sum_{i=H^0,h^0,G^0,A^0}\eta_i^{(3)}\{\eta^{(1)}[6(D_{27}-D_{311})+m_b^2(D_{11}-2D_{12}-2D_{22}-2D_{36}+(1+\zeta_i)(D_0+D_{12}))$$
$$-m_t^2(2D_{23}+2D_{37}+(1+\zeta_i)D_{13})-2p_b\cdot k(D_{12}+2D_{24}+2D_{34})+2p_t\cdot k(D_{13}+2D_{25}+2D_{35})$$
$$+2p_t\cdot p_b(D_{13}+2D_{26}+D_{310})]+\eta^{(2)}m_tm_b(1+\zeta_i)(D_{12}-D_{13}-D_0)\}(-k,-p_b,p_t,m_b,m_b,m_i,m_t),$$

$$f_8^{b(s)}=f_7^{b(s)}(\eta^{(1)}\leftrightarrow\eta^{(2)}),$$

$$f_9^{b(s)}=\sum_{i=H^0,h^0,G^0,A^0}\eta_i^{(3)}\{\eta^{(1)}2m_t[-D_{13}-D_{26}+(1+\zeta_i)(D_{12}+D_{24})]+\eta^{(2)}2m_b[-D_{22}+D_{24}+\zeta_i(D_0+2D_{12}+D_{24})]\}$$
$$\times(-k,-p_b,p_t,m_b,m_b,m_i,m_t)-\frac{8\sqrt{2}m_W}{\sin 2\beta}\sum_{i,j,k}\sigma_{ij}N_{k4}N_{k3}^*R_i(b)R_j(t)(D_{12}+D_{24})$$
$$\times(-k,-p_b,p_t,m_{\tilde{b}_i},m_{\tilde{b}_i},m_{\tilde{\chi}_k^0},m_{\tilde{t}_j}),$$

$$f_{10}^{b(s)}=f_9^{b(s)}(\eta^{(1)}\leftrightarrow\eta^{(2)},L_l\leftrightarrow R_l,N_{kl}\leftrightarrow N_{kl}^*),$$

$$f_{11}^{b(s)}=\sum_{i=H^0,h^0,G^0,A^0}\eta_i^{(3)}\{\eta^{(1)}2m_t[D_{23}-(1+\zeta_i)D_{25}]-\eta^{(2)}2m_b[-D_{26}+D_{25}+\zeta_i(D_{13}+D_{25})]\}$$
$$\times(-k,-p_b,p_t,m_b,m_b,m_i,m_t)+\frac{8\sqrt{2}m_W}{\sin 2\beta}\sum_{i,j,k}\sigma_{ij}N_{k4}N_{k3}^*R_i(b)R_j(t)(D_{13}+D_{25})$$
$$\times(-k,-p_b,p_t,m_{\tilde{b}_i},m_{\tilde{b}_i},m_{\tilde{\chi}_k^0},m_{\tilde{t}_j}),$$

$$f_{12}^{b(s)}=f_{11}^{b(s)}(\eta^{(1)}\leftrightarrow\eta^{(2)},L_l\leftrightarrow R_l,N_{kl}\leftrightarrow N_{kl}^*),$$

where D_0,D_{ij},D_{ijk} are the four-point Feynman integrals [19]. The explicit forms of $\delta M^{V_1(t)},\delta M^{s(t)},\delta M^{b(t)}$, can be, respectively, obtained from $\delta M^{V_1(s)},\delta M^{s(s)},\delta M^{b(s)}$ by the transformation U, which is defined as

$$p_b\rightarrow p_t,\quad \hat{s}\rightarrow\hat{t},\quad k\rightarrow -k,\quad \xi_i^{(1)}\rightarrow\xi_i^{(2)},\quad \xi_i^{(3)}\rightarrow\xi_i^{(4)},\quad \eta_i^{(1)}\rightarrow\eta_i^{(2)},$$
$$m_t\leftrightarrow m_b,\quad \eta^{(1)}\leftrightarrow\eta^{(2)},\quad \lambda_b\leftrightarrow\lambda_t,\quad m_{\tilde{t}_i}\leftrightarrow m_{\tilde{b}_i},\quad U_{i2}\leftrightarrow V_{i2}^*,\quad N_{i3}\leftrightarrow N_{i4}^*,$$
$$L_i(b)\leftrightarrow L_i(t),\quad R_i(b)\leftrightarrow R_i(t),\quad p_b^\mu P_{L(R)}\leftrightarrow p_t^\mu P_{R(L)},\quad \gamma^\mu\not{k}P_L\leftrightarrow\gamma^\mu\not{k}P_R.$$

All other form factors f_i^l not listed above vanish. In the above expressions we have used the following definitions:

$$\eta^{(1)}=m_b\tan\beta,\quad \eta^{(2)}=m_t\cot\beta,\quad \lambda_b=\frac{m_b}{\sqrt{2}m_W\cos\beta},\quad \lambda_t=\frac{m_t}{\sqrt{2}m_W\sin\beta}$$

$$L_1(q)=\cos\theta_q,\quad L_2(q)=-\sin\theta_q,\quad R_1(q)=\sin\theta_q,\quad R_2(q)=\cos\theta_q,$$

$$\eta_{H^0}^{(1)}=\frac{\cos^2\alpha}{\cos^2\beta},\quad \eta_{h^0}^{(1)}=\frac{\sin^2\alpha}{\cos^2\beta},\quad \eta_{A^0}^{(1)}=\tan^2\beta,\quad \eta_{G^0}^{(1)}=1,$$

$$\eta_{H^0}^{(2)}=\frac{\sin^2\alpha}{\sin^2\beta},\quad \eta_{h^0}^{(2)}=\frac{\cos^2\alpha}{\sin^2\beta},\quad \eta_{A^0}^{(2)}=\cot^2\beta,\quad \eta_{G^0}^{(2)}=1,$$

$$\eta_{H^0}^{(3)}=-\eta_{h^0}^{(3)}=\frac{\sin\alpha\cos\alpha}{\sin\beta\cos\beta},\quad \eta_{G^0}^{(3)}=-\eta_{A^0}^{(3)}=1,$$

$$\xi_{H^-}^{(1)}=\frac{m_t^2}{m_b^2}\cot^2\beta,\quad \xi_{G^-}^{(1)}=\frac{m_t^2}{m_b^2},\quad \xi_{H^-}^{(2)}=\frac{m_b^2}{m_t^2}\tan^2\beta,\quad \xi_{G^-}^{(2)}=\frac{m_b^2}{m_t^2},$$

$$\xi^{(3)}_{H^-}=\tan^2\beta,\quad \xi^{(3)}_{G^-}=1,\quad \xi^{(4)}_{H^-}=\cot^2\beta,\quad \xi^{(4)}_{G^-}=1,$$

$$\zeta_{H^0}=\zeta_{h^0}=\zeta_{H^-}=-\zeta_{A^0}=-\zeta_{G^0}=-\zeta_{G^-}=1,$$

$$\sigma_{ij}=\frac{m_W}{\sqrt{2}}\left(\sin 2\beta-\frac{m_b^2\tan\beta+m_t^2\cot\beta}{m_W^2}\right)L_i(b)L_j(t)+\frac{m_t m_b}{\sqrt{2}m_W}(\tan\beta+\cot\beta)R_i(b)R_j(t)$$
$$-\frac{m_b}{\sqrt{2}m_W}(\mu-A_b\tan\beta)R_i(b)L_j(t)-\frac{m_t}{\sqrt{2}m_W}(\mu-A_t\cot\beta)L_i(b)R_j(t),$$

$$g_1^{V_1(s)}=\sum_{i=H^0,h^0,G^0,A^0}\eta_i^{(1)}\left\{\left[\frac{1}{2}-2\overline{C}_{24}+m_b^2(-2C_{11}+C_{12}-C_{21}+C_{23})-\hat{s}(C_{12}+C_{23})\right](-p_b,-k,m_i,m_b,m_b)\right.$$
$$\left.+[-F_0+F_1+2m_b^2G_1-(1+\zeta_i)2m_b^2G_0](m_b^2,m_i,m_b)\right\},$$

$$g_2^{V_1(s)}=\sum_{i=H^-,G^-}2\left\{\xi_i^{(1)}\left[\frac{1}{2}-2\overline{C}_{24}+m_t^2C_0+m_b^2(-C_0-2C_{11}+C_{12}-C_{21}+C_{23})-\hat{s}(C_{12}+C_{23})\right]\right.$$
$$\left.\times(-p_b,-k,m_i,m_t,m_t)+[\xi_i^{(1)}(-F_0+F_1)-2m_t^2\zeta_iG_0+m_b^2(\xi_i^{(1)}+\xi_i^{(3)})(G_1-\zeta_iG_0)](m_b^2,m_i,m_t)\right\}$$
$$+\frac{4m_W^2}{m_b^2}\sum_{i,j}\{\lambda_b^2[R_j^2(b)|N_{i3}|^2(-F_0+F_1)+m_b^2|N_{i3}|^2(-G_0+G_1)-2m_bm_{\tilde{\chi}_i^0}L_j(b)R_j(b)N_{i3}^{*2}G_0]$$
$$\times(m_b^2,m_{\tilde{b}_j},m_{\tilde{\chi}_i^0})+[-2m_bm_{\tilde{\chi}_i^+}\lambda_b\lambda_tL_j(t)R_j(t)V_{i2}^{*2}U_{i2}^{*2}G_0+\lambda_t^2R_j^2(t)|V_{i2}|^2(-F_0+F_1)$$
$$+m_b^2(\lambda_t^2R_j^2(t)|V_{i2}|^2+\lambda_b^2L_j^2(t)|U_{i2}|^2)(-G_0+G_1)](m_b^2,m_{\tilde{t}_j},m_{\tilde{\chi}_i^+})-2\lambda_b^2R_j^2(b)|N_{i3}|^2\overline{C}_{24}$$
$$\times(-p_b,-k,m_{\tilde{\chi}_i^0},m_{\tilde{b}_j},m_{\tilde{b}_j})-2\lambda_t^2R_j^2(t)|V_{i2}|^2\overline{C}_{24}(-p_b,-k,m_{\tilde{\chi}_i^+},m_{\tilde{t}_j},m_{\tilde{t}_j})\},$$

$$g_3^{V_1(s)}=g_2^{V_1(s)}[\xi_i^{(1)}\leftrightarrow\xi_i^{(3)},V_{i2}\leftrightarrow U_{i2}^*,N_{i3}\leftrightarrow N_{i3}^*,L_j(b)\leftrightarrow R_j(b),\lambda_bL_j(t)\leftrightarrow\lambda_tR_j(t)],$$

$$g_4^{V_1(s)}=\sum_{i=H^0,h^0,G^0,A^0}\eta_i^{(1)}2m_b[C_0+2C_{11}+C_{21}+\zeta_i(C_0+C_{11})](-p_b,-k,m_i,m_b,m_b)$$
$$+\sum_{i=H^-,G^-}4m_b\left[\xi_i^{(3)}(C_0+2C_{11}+C_{21})+\frac{m_t^2}{m_b^2}\zeta_i(C_0+C_{11})\right](-p_b,-k,m_i,m_t,m_t)$$
$$+\frac{8m_W^2}{m_b^2}\sum_{i,j}\{\lambda_b^2[m_{\tilde{\chi}_i^0}L_j(b)R_j(b)N_{i3}^{*2}(C_0+C_{11})-m_bL_j^2(b)|N_{i3}|^2(C_{11}+C_{21})](-p_b,-k,m_{\tilde{\chi}_i^0},m_{\tilde{b}_j},m_{\tilde{b}_j})$$
$$+[m_{\tilde{\chi}_i^+}\lambda_b\lambda_tL_j(t)R_j(t)V_{i2}^*U_{i2}^*(C_0+C_{11})-m_b\lambda_b^2L_j^2(t)|U_{i2}|^2(C_{11}+C_{21})](-p_b,-k,m_{\tilde{\chi}_i^+},m_{\tilde{t}_j},m_{\tilde{t}_j})\},$$

$$g_5^{V_1(s)}=g_4^{V_1(s)}[\xi_i^{(1)}\leftrightarrow\xi_i^{(3)},V_{i2}\leftrightarrow U_{i2}^*,N_{i3}\leftrightarrow N_{i3}^*,L_j(b)\leftrightarrow R_j(b),\lambda_bL_j(t)\leftrightarrow\lambda_tR_j(t)],$$

$$g_6^{V_1(s)}=-\sum_{i=H^0,h^0,G^0,A^0}\eta_i^{(1)}m_b(C_0+C_{11}+\zeta_iC_0)(-p_b,-k,m_i,m_b,m_b)-\sum_{i=H^-,G^-}2m_b$$
$$\times\left[\xi_i^{(3)}(C_0+C_{11})+\frac{m_t^2}{m_b^2}\zeta_iC_0\right](-p_b,-k,m_i,m_t,m_t),$$

$$g_7^{V_1(s)}=g_6^{V_1(s)}(\xi_i^{(1)}\leftrightarrow\xi_i^{(3)}),$$

$$g_8^{V_1(s)} = \sum_{i=H^0,h^0,G^0,A^0} 2\eta_i^{(1)}(C_{12}+C_{23})(-p_b,-k,m_i,m_b,m_b) + \sum_{i=H^-,G^-} 4\xi_i^{(1)}(C_{12}+C_{24})(-p_b,-k,m_i,m_t,m_t)$$
$$-\frac{8m_W^2}{m_b^2}\sum_{i,j}\{\lambda_b^2 R_j^2(b)|N_{i3}|^2(C_{12}+C_{23})(-p_b,-k,m_{\tilde{\chi}_i^0},m_{\tilde{b}_j},m_{\tilde{b}_j}) + \lambda_t^2 R_j^2(t)|V_{i2}|^2(C_{12}+C_{23})$$
$$\times(-p_b,-k,m_{\tilde{\chi}_i^+},m_{\tilde{t}_j},m_{\tilde{t}_j})\},$$

$$g_9^{V_1(s)} = g_8^{V_1(s)}[\xi_i^{(1)} \leftrightarrow \xi_i^{(3)}, V_{i2}\leftrightarrow U_{i2}^*, N_{i3}\leftrightarrow N_{i3}^*, L_j(b)\leftrightarrow R_j(b), \lambda_b L_j(t)\leftrightarrow \lambda_t R_j(t)],$$

$$g_1^{V_2(s)} = \sum_{i=H^0,h^0,G^0,A^0} \eta_i^{(3)}\left\{\eta^{(1)}\left[-\frac{1}{2}+4\bar{C}_{24}+m_t^2(C_0+2C_{11}+\zeta_i(C_0+C_{11})+C_{21}-C_{12}-C_{23})\right.\right.$$
$$\left.\left.+m_{H^-}^2(C_{22}-C_{23})+\hat{s}(C_{12}+C_{23})\right]+\eta^{(2)}m_b m_t[\zeta_i C_{11}+(1+\zeta_i)C_0]\right\}(-p_t,-p_{H^-},m_i,m_t,m_b)$$
$$+\frac{4\sqrt{2}m_W}{\sin 2\beta}\sum_{i,j,k}[m_t R_i(b)R_j(t)N_{k3}^* N_{k4}(-C_{11}+C_{12})+m_{\tilde{\chi}_k^0}L_j(t)R_i(b)N_{k3}^* N_{k4}^* C_0]\sigma_{ij}$$
$$\times(-p_t,-p_{H^-},m_{\tilde{\chi}_k^0},m_{\tilde{b}_i},m_{\tilde{t}_j}),$$

$$g_2^{V_2(s)} = g_1^{V_2(s)}(\eta^{(1)}\leftrightarrow\eta^{(2)}, L_l\leftrightarrow R_l, N_{kl}\leftrightarrow N_{kl}^*),$$

$$g_3^{V_2(s)} = \sum_{i=H^0,h^0,G^0,A^0} \eta_i^{(3)}\{\eta^{(1)}m_t[C_0+C_{11}+\zeta_i(C_0+C_{12})]+\eta^{(2)}\zeta_i m_b C_{12}\}(-p_t,-p_{H^-},m_i,m_t,m_b)$$
$$-\frac{4\sqrt{2}m_W}{\sin 2\beta}\sum_{i,j,k}R_i(b)R_j(t)N_{k3}^* N_{k4}\sigma_{ij}C_{12}(-p_t,-p_{H^-},m_{\tilde{\chi}_k^0},m_{\tilde{b}_i},m_{\tilde{t}_j}),$$

$$g_4^{V_2(s)} = g_3^{V_2(s)}(\eta^{(1)}\leftrightarrow\eta^{(2)}, L_l\leftrightarrow R_l, N_{kl}\leftrightarrow N_{kl}^*),$$

$$g_1^{V_2(t)} = \sum_{i=H^0,h^0,G^0,A^0} \eta_i^{(3)}\left\{\eta^{(1)}\left[-\frac{1}{2}+4\bar{C}_{24}+m_b^2(C_0+2C_{11}+\zeta_i(C_0+C_{11})+C_{21}-C_{12}-C_{23})+m_{H^-}^2(C_{22}-C_{23})\right.\right.$$
$$\left.\left.+\hat{t}(C_{12}+C_{23})\right]+\eta^{(2)}m_b m_t[C_0+\zeta_i(C_0+C_{11})]\right\}(-p_b,p_{H^-},m_i,m_b,m_t)$$
$$+\frac{4\sqrt{2}m_W}{\sin 2\beta}\sum_{i,j,k}[m_b L_i(b)L_j(t)N_{k3}^* N_{k4}(-C_{11}+C_{12})+m_{\tilde{\chi}_k^0}L_j(t)R_i(b)N_{k3}^* N_{k4}^* C_0]\sigma_{ij}$$
$$\times(-p_b,p_{H^-},m_{\tilde{\chi}_k^0},m_{\tilde{b}_i},m_{\tilde{t}_j}),$$

$$g_2^{V_2(t)} = g_1^{V_2(t)}(\eta^{(1)}\leftrightarrow\eta^{(2)}, L_l\leftrightarrow R_l, N_{kl}\leftrightarrow N_{kl}^*),$$

$$g_3^{V_2(t)} = -\sum_{i=H^0,h^0,G^0,A^0} \eta_i^{(3)}\{\eta^{(1)}m_b[C_0+C_{11}+\zeta_i(C_0+C_{12})]+\eta^{(2)}\zeta_i m_t C_{12}\}(-p_b,p_{H^-},m_i,m_b,m_t)$$
$$+\frac{4\sqrt{2}m_W}{\sin 2\beta}\sum_{i,j,k}R_i(b)R_j(t)N_{k3}^* N_{k4}\sigma_{ij}C_{12}(-p_b,p_{H^-},m_{\tilde{\chi}_k^0},m_{\tilde{b}_i},m_{\tilde{t}_j}),$$

$$g_4^{V_2(t)} = g_3^{V_2(t)}(\eta^{(1)}\leftrightarrow\eta^{(2)}, L_l\leftrightarrow R_l, N_{kl}\leftrightarrow N_{kl}^*),$$

$$g_1^{s(s)}=\sum_{i=H^0,h^0,G^0,A^0} m_b\eta_i^{(1)}\{-\zeta_iF_0(p_b+k,m_i,m_b)+[\zeta_iF_0-2m_b^2(1+\zeta_i)G_0+2m_b^2G_1](m_b^2,m_i,m_b)\}$$
$$+\sum_{i=H^-,G^-} 2m_b\Bigg\{-\frac{m_t^2}{m_b^2}\zeta_iF_0(p_b+k,m_i,m_t)+\Bigg[-2m_t^2\zeta_iG_0+m_b^2(\xi_i^{(1)}+\xi_i^{(3)})(G_1-\zeta_iG_0)+\zeta_i\frac{m_t^2}{m_b^2}F_0\Bigg]$$
$$\times(m_b^2,m_i,m_t)\Bigg\}+\frac{4m_W^2}{m_b^2}\sum_{i,j}\{-m_{\tilde{\chi}_i^0}\lambda_b^2L_j(b)R_j(b)N_{i3}^{*2}F_0(p_b+k,m_{\tilde{b}_j},m_{\tilde{\chi}_i^0})$$
$$-m_{\tilde{\chi}_i^+}\lambda_b\lambda_tL_j(b)R_j(b)V_{i2}^*U_{i2}^*F_0(p_b+k,m_{\tilde{t}_j},m_{\tilde{\chi}_i^+})+[m_b^3\lambda_b^2|N_{i3}|^2(-G_0+G_1)$$
$$-m_{\tilde{\chi}_i^0}\lambda_b^2L_j(b)R_j(b)N_{i3}^{*2}(2m_b^2G_0-F_0)](m_b^2,m_{\tilde{b}_j},m_{\tilde{\chi}_i^0})+[m_b^3(\lambda_b^2L_j^2(t)|U_{i2}|^2+\lambda_t^2R_j^2(t)|V_{i2}|^2)$$
$$\times(-G_0+G_1)-m_{\tilde{\chi}_i^+}\lambda_b\lambda_tL_j(t)R_j(t)V_{i2}^*U_{i2}^*(2m_b^2G_0-F_0)](m_b^2,m_{\tilde{t}_j},m_{\tilde{\chi}_i^+})\},$$

$$g_2^{s(s)}=\sum_{i=H^0,h^0,G^0,A^0}\eta_i^{(1)}(-F_0+F_1)(p_b+k,m_i,m_b),$$

$$g_3^{s(s)}=\sum_{i=H^0,h^0,G^0,A^0}\eta_i^{(1)}[F_0-F_1-2m_b^2G_1+2(1+\zeta_i)m_b^2G_0](m_b^2,m_i,m_b)$$
$$+\sum_{i=H^-,G^-}2\{\xi_i^{(1)}(-F_0+F_1)(p_b+k,m_i,m_t)-[\xi_i^{(1)}(-F_0+F_1)-2\zeta_im_t^2G_0+m_b^2(\xi_i^{(1)}+\xi_i^{(3)})(G_1-\zeta_iG_0)]$$
$$\times(m_b^2,m_i,m_t)\}-\frac{4m_W^2}{m_b^2}\sum_{i,j}\{\lambda_b^2[R_j^2(b)|N_{i3}|^2(-F_0+F_1)+|N_{i3}|^2m_b^2(-G_0+G_1)$$
$$-2m_bm_{\tilde{\chi}_i^0}L_j(b)R_j(b)N_{i3}^{*2}G_0](m_b^2,m_{\tilde{b}_j},m_{\tilde{\chi}_i^0})+[\lambda_t^2R_j^2(t)|V_{i2}|^2(-F_0+F_1)+m_b^2(\lambda_t^2R_j^2(t)|V_{i2}|^2$$
$$+\lambda_b^2L_j^2(t)|U_{i2}|^2)(G_1-G_0)-2m_bm_{\tilde{\chi}_i^+}L_j(t)R_j(t)\lambda_b\lambda_tV_{i2}^*U_{i2}^*G_0](m_b^2,m_{\tilde{t}_j},m_{\tilde{\chi}_i^+})-\lambda_b^2R_j^2(b)|N_{i3}|^2$$
$$\times(-F_0+F_1)(p_b+k,m_{\tilde{b}_j},m_{\tilde{\chi}_i^0})-\lambda_t^2R_j^2(t)|V_{i2}|^2(-F_0+F_1)(p_b+k,m_{\tilde{t}_j},m_{\tilde{\chi}_i^+})\},$$

$$g_4^{s(s)}=g_3^{s(s)}[\xi_i^{(1)}\leftrightarrow\xi_i^{(3)},V_{i2}\leftrightarrow U_{i2}^*,N_{i3}\leftrightarrow N_{i3}^*,L_j(b)\leftrightarrow R_j(b),\lambda_bL_j(t)\leftrightarrow\lambda_tR_j(t)],$$

$$g_5^{s(s)}=g_1^{s(s)}(N_{i3}^*\to N_{i3},V_{i2}^*\to V_{i2},U_{i2}^*\to U_{i2}),$$

$$\delta\Lambda_L^{(1)}=\frac{4N_c}{3m_W^2}(1-\cot^2\theta_W)\Bigg[2m_t^2\Bigg(\ln\frac{m_t^2}{\mu^2}-1\Bigg)+m_b^2+m_t^2-\frac{5}{6}m_W^2+m_b^2F_0+(m_b^2-m_t^2-2m_W^2)F_1\Bigg]$$
$$\times(m_W^2,m_b,m_t)+\frac{4N_c}{3m_W^2}\cot^2\theta_W\Bigg\{-\frac{5}{6}[(g_V^b)^2+(g_A^b)^2+(g_V^t)^2+(g_A^t)^2]m_Z^2$$
$$+\Bigg[((g_V^t)^2+(g_A^t)^2)\Bigg(2m_t^2\ln\frac{m_t^2}{\mu^2}+m_t^2F_0-2m_Z^2F_1\Bigg)-((g_V^t)^2-(g_A^t)^2)3m_t^2F_0\Bigg](m_Z^2,m_t,m_t)$$
$$+\Bigg[((g_V^b)^2+(g_A^b)^2)\Bigg(2m_b^2\ln\frac{m_b^2}{\mu^2}+m_b^2F_0-2m_Z^2F_1\Bigg)-((g_V^b)^2-(g_A^b)^2)3m_b^2F_0\Bigg](m_Z^2,m_b,m_b)\Bigg\}$$
$$+\frac{4N_c}{m_W^2}[(\cot^2\beta-1)m_t^2F_0+(m_t^2-m_b^2-2m_t^2\cot^2\beta)F_1+(m_t^2\cot^2\beta+m_b^2\tan^2\beta+2m_b^2)m_t^2G_0$$
$$-(m_t^2\cot^2\beta+m_b^2\tan^2\beta)m_{H^-}^2G_1](m_{H^-}^2,m_t,m_b)+\sum_{i=H^0,h^0,G^0,A^0}\frac{1}{2m_W^2}\{m_b^2\eta_i^{(1)}[F_1-F_0-2m_b^2$$

$$\times(G_0+\zeta_i G_0-G_1)](m_b^2,m_i,m_b)-m_t^2\eta_i^{(2)}[-(1+2\zeta_i)F_0+F_1+2m_t^2(1+\zeta_i)G_0-2m_t^2G_1](m_t^2,m_i,m_t)\}$$

$$+\sum_{i=H^-,G^-}\frac{1}{m_W^2}\Bigg\{m_b^2[\xi_i^{(1)}(-F_0+F_1)-2m_t^2\zeta_iG_0+m_b^2(\xi_i^{(1)}+\xi_i^{(3)})(G_1-\zeta_iG_0)](m_b^2,m_i,m_t)$$

$$-m_t^2\left[-\frac{2m_b^2}{m_t^2}\zeta_iF_0+\xi_i^{(2)}(-F_0+F_1)+2m_b^2\zeta_iG_0-m_t^2(\xi_i^{(2)}+\xi_i^{(4)})(G_1-\zeta_iG_0)\right](m_t^2,m_i,m_b)\Bigg\}$$

$$-2N_C\sum_{i,j}\Bigg\{2\sigma_{ij}\sigma_{ij}G_0+\frac{1}{m_W^2}L_i(b)L_j(t)\Bigg[L_i(b)L_j(t)\left(\frac{m_b^2}{\cos^2\beta}+\frac{m_t^2}{\sin^2\beta}\right)\cos2\beta$$

$$+R_i(b)R_j(t)m_tm_b(\tan^2\beta-\cot^2\beta)\Bigg]\Bigg\}(m_{H^-}^2,m_{\tilde{t}_j},m_{\tilde{b}_i}),$$

$$\delta\Lambda_L^{(2)}=-2\sum_{i,j}\Bigg\{\lambda_t^2\left[-\frac{2m_{\tilde{\chi}_i^0}}{m_t}L_j(t)R_j(t)N_{i4}^{*2}(F_0-m_t^2G_0)+|N_{i4}|^2[R_j^2(t)(-F_0+F_1)-m_t^2(-G_0+G_1)]\right]$$

$$\times(m_t^2,m_{\tilde{t}_j},m_{\tilde{\chi}_i^0})+\Bigg[-\frac{2m_{\tilde{\chi}_i^+}}{m_t}\lambda_b\lambda_tL_j(b)R_j(b)U_{i2}^*V_{i2}^*(F_0-m_t^2G_0)+\lambda_b^2R_j^2(b)|U_{i2}|^2(-F_0+F_1)$$

$$-m_t^2[\lambda_t^2L_j^2(b)|V_{i2}|^2+\lambda_b^2R_j^2(b)|U_{i2}|^2](-G_0+G_1)\Bigg](m_t^2,m_{\tilde{b}_j},m_{\tilde{\chi}_i^+})\Bigg\},$$

$$\delta\Lambda_L^{(3)}=2\sum_{i,j}\{\lambda_b^2[|Ni3|^2(R_j^2(b)(-F_0+F_1)+m_b^2(-G_0+G_1))-2m_bm_{\tilde{\chi}_i^0}L_j(b)R_j(b)N_{i3}^{*2}G_0](m_b^2,m_{\tilde{b}_j},m_{\tilde{\chi}_i^0})$$

$$+[-2m_{\tilde{\chi}_i^+}m_b\lambda_b\lambda_tL_j(t)R_j(t)U_{i2}^*V_{i2}^*G_0+\lambda_b^2L_j^2(b)|U_{i2}|^2(-F_0+F_1)+m_b^2(\lambda_t^2R_j^2(t)|V_{i2}|^2$$

$$+\lambda_b^2L_j^2(t)|U_{i2}|^2)(-G_0+G_1)](m_b^2,m_{\tilde{t}_j},m_{\tilde{\chi}_i^+})\},$$

$$\delta\Lambda_R^{(1)}=\sum_{i=H^0,h^0,G^0,A^0}\frac{1}{2m_W^2}\{m_t^2\eta_i^{(2)}[-F_0+F_1-2m_t^2(G_0+\zeta_iG_0-G_1)](m_t^2,m_i,m_t)-m_b^2\eta_i^{(1)}$$

$$\times[-F_0+F_1-2\zeta_iF_0+2m_b^2(1+\zeta_i)G_0-2m_b^2G_1](m_b^2,m_i,m_b)\}$$

$$+\sum_{i=H^-,G^-}\frac{1}{m_W^2}\Bigg\{m_t^2[\xi_i^{(2)}(-F_0+F_1)-2m_b^2\zeta_iG_0+m_t^2(\xi_i^{(2)}+\xi_i^{(4)})(G_1-\zeta_iG_0)](m_t^2,m_i,m_b)$$

$$-m_b^2\left[-\frac{2m_t^2}{m_b^2}\zeta_iF_0+\xi_i^{(1)}(-F_0+F_1)+2m_t^2\zeta_iG_0-m_b^2(\xi_i^{(1)}+\xi_i^{(3)})(G_1-\zeta_iG_0)\right](m_b^2,m_i,m_t)\Bigg\},$$

$$\delta\Lambda_R^{(2)}=\delta\Lambda_L^{(2)}(U),\quad \delta\Lambda_R^{(3)}=\delta\Lambda_L^{(3)}(U).$$

Here C_0,C_{ij} are the three-point Feynman integrals [19] and $\overline{C_{24}}\equiv-\frac{1}{4}\Delta+C_{24}$, while

$$F_n(q,m_1,m_2)=\int_0^1dy\,y^n\ln\left[\frac{-q^2y(1-y)+m_1^2(1-y)+m_2^2y}{\mu^2}\right],$$

$$G_n(q,m_1,m_2)=-\int_0^1dy\,\frac{y^{n+1}(1-y)}{-q^2y(1-y)+m_1^2(1-y)+m_2^2y},$$

and

$$g_V^t=\frac{1}{2}-\frac{4}{3}\sin^2\theta_W, \quad g_A^t=\frac{1}{2}, \quad g_V^b=-\frac{1}{2}+\frac{2}{3}\sin^2\theta_W, \quad g_A^b=-\frac{1}{2},$$

which are the SM couplings of the top and bottom quarks to the Z boson. The definitions of $\theta_q, U_{ij}, V_{ij}, N_{ij}, \mu$, and A_q can be found in Ref. [2].

APPENDIX B

$$h_1^{(i)}=4m_t\eta^{(2)}(2p_b\cdot k-p^{(i)}\cdot p_b)-4m_b\eta^{(1)}(p^{(i)}\cdot p_t+p_t\cdot k),$$

$$h_2^{(i)}=h_1^{(i)}(\eta^{(1)}\leftrightarrow\eta^{(2)}),$$

$$h_3^{(i)}=2\eta^{(2)}(2p_b\cdot kp_b\cdot p_t-m_b^2p_t\cdot k-2p^{(i)}\cdot p_bp_b\cdot p_t)+2m_bm_t\eta^{(1)}(p_b\cdot k-2p^{(i)}\cdot p_b),$$

$$h_4^{(i)}=h_3^{(i)}(\eta^{(1)}\leftrightarrow\eta^{(2)}),$$

$$h_5^{(i)}=2\eta^{(2)}(m_t^2p_b\cdot k-2p^{(i)}\cdot p_tp_b\cdot p_t)+2m_bm_tm_t\eta^{(1)}(p_t\cdot k-2p^{(i)}\cdot p_t),$$

$$h_6^{(i)}=h_5^{(i)}(\eta^{(1)}\leftrightarrow\eta^{(2)}),$$

$$h_7^{(i)}=4\eta^{(2)}(p^{(i)}\cdot p_bp_t\cdot k-p^{(i)}\cdot kp_b\cdot p_t-p_b\cdot kp^{(i)}\cdot p_t-2p_b\cdot kp_t\cdot k)-4m_bm_t\eta^{(1)}p^{(i)}\cdot k,$$

$$h_8^{(i)}=h_7^{(i)}(\eta^{(1)}\leftrightarrow\eta^{(2)}),$$

$$h_9^{(i)}=4m_t\eta^{(2)}p_b\cdot k(p_b\cdot k-p^{(i)}\cdot p_b)-4m_b\eta^{(1)}p^{(i)}\cdot p_bp_t\cdot k,$$

$$h_{10}^{(i)}=h_9^{(i)}(\eta^{(1)}\leftrightarrow\eta^{(2)}),$$

$$h_{11}^{(i)}=4m_t\eta^{(2)}p_b\cdot k(p_t\cdot k-p^{(i)}\cdot p_t)-4m_b\eta^{(1)}p_t\cdot kp^{(i)}\cdot p_t,$$

$$h_{12}^{(i)}=h_{11}^{(i)}(\eta^{(1)}\leftrightarrow\eta^{(2)}),$$

where the index i represents the two channels s and t, and $p^{(s)}=p_b$, $p^{(t)}=p_t$.

[1] For a review, see J. Gunion, H. Haber, G. Kane, and S. Dawson, *The Higgs Hunter's Guide* (Addison-Wesley, New York, 1990).

[2] H.E. Haber and G.L. Kane, Phys. Rep. **117**, 75 (1985); J.F. Gunion and H.E. Haber, Nucl. Phys. **B272**, 1 (1986).

[3] E. Eichten, I. Hinchliffe, K. Lane, and C. Quigg, Rev. Mod. Phys. **56**, 579 (1984); **56**, 1065(E) (1986); N.G. Deshpande, X. Tata, and D.A. Dicus, Phys. Rev. D **29**, 1527 (1984); S. Willenbrock, *ibid.* **35**, 173 (1987); A. Krause, T. Plehn, M. Spria, and P.M. Zerwas, Nucl. Phys. **B519**, 85 (1998); J. Yi, M. Wen-Gan, H. Liang, H. Meng, and Y. Zeng-Hui, J. Phys. G **23**, 385 (1997); **23**, 1151(E) (1997).

[4] D.A. Dicus, J.L. Hewett, C. Kao, and T.G. Rizzo, Phys. Rev. D **40**, 787 (1989); A.A. Barrientos Bendezú and B.A. Kniehl, *ibid.* **59**, 015009 (1999).

[5] S. Moretti and K. Odagiri, Phys. Rev. D **59**, 055008 (1999).

[6] Z. Kunszt and F. Zwirner, Nucl. Phys. **B385**, 3 (1992), and references cited therein.

[7] J.F. Gunion, H.E. Haber, F.E. Paige, W.-K. Tung, and S. Willenbrock, Nucl. Phys. **B294**, 621 (1987); R.M. Barnett, H.E. Haber, and D.E. Soper, *ibid.* **B306**, 697 (1988); F.I. Olness and W.-K. Tung, *ibid.* **B308**, 813 (1988).

[8] V. Barger, R.J.N. Phillips, and D.P. Roy, Phys. Lett. B **324**, 236 (1994).

[9] C.S. Huang and S.H. Zhu, Phys. Rev. D **60**, 075012 (1999).

[10] K. Odagiri, hep-ph/9901432; Phys. Lett. B **452**, 327 (1999).

[11] D.P. Roy, Phys. Lett. B **459**, 607 (1999).

[12] Francesca Borzumati, Jean-Loic Kneur, and Nir Polonsky, Phys. Rev. D **60**, 115011 (1999).

[13] S. Sirlin, Phys. Rev. D **22**, 971 (1980); W.J. Marciano and A. Sirlin, *ibid.* **22**, 2695 (1980); **31**, 213(E) (1985); A. Sirlin and W.J. Marciano, Nucl. Phys. **B189**, 442 (1981); K.I. Aoki *et al.*, Suppl. Prog. Theor. Phys. **73**, 1 (1982).

[14] A. Mendez and A. Pomarol, Phys. Lett. B **279**, 98 (1992).

[15] Particle Data Group, C. Caso *et al.*, Eur. Phys. J. C **3**, 1 (1998).

[16] J. Gunion and A. Turski, Phys. Rev. D **39**, 2701 (1989); **40**, 2333 (1990); J.R. Espinosa and M. Quiros, Phys. Lett. B **266**, 389 (1991); M. Carena, M. Quiros, and C.E.M. Wagner, Nucl. Phys. **B461**, 407 (1996).

[17] CTEQ Collaboration, H.L. Lai *et al.*, Eur. Phys. J. D **12**, 375 (2000).

[18] C.S. Li, R.J. Oakes, and J.M. Yang, Phys. Rev. D **55**, 5780 (1997).

[19] G. Passarino and M. Veltman, Nucl. Phys. **B160**, 151 (1979); A. Axelrod, *ibid.* **B209**, 349 (1982); M. Clements *et al.*, Phys. Rev. D **27**, 570 (1983).